Relaxation and dephasing quantum kinetics for a quantum dot in an optically excited quantum well

Q. T. Vu,[1,2] H. Haug,[1] and S. W. Koch[2]
[1]*Institut für Theoretische Physik, J.W. Goethe-Universität Frankfurt, Max-von-Laue-Strasse 1, D-60438 Frankfurt am Main, Germany*
[2]*Fachbereich Physik und Wissenschaftliches Zentrum für Materialwissenschaften, Philipps-Universität Marburg, Renthof 5, D-35037 Marburg, Germany*
(Received 17 August 2005; revised manuscript received 5 January 2006; published 9 May 2006)

We investigate the population and dephasing kinetics of a quantum dot coupled by Auger and phonon scattering processes with a femtosecond-pulse-excited electron-hole plasma in a quantum well or wetting layer. For the two-dimensional (2D) plasma we treat the quantum kinetics of the Coulomb scattering processes with a two-time-dependent screened Coulomb interaction potential. Additionally the scattering with LO phonons is included. For ultrashort pulse excitations close to the band edge of the plasma we obtain a slow decay of the polarization of the quantum dot with superimposed oscillations whose frequency is given by the energetic distance of the quantum dot levels and the 2D band edge. For two-pulse excitations we calculate the absorption spectrum of the probe pulse for various delay times and pump pulse intensities. One sees, e.g., the buildup of gain for a strong pump pulse in the spectral regions below the dot absorption line and below the band edge of the plasma. In the calculated four-wave-mixing signal we find in addition to long dephasing times, which decrease with increasing 2D plasma densities, also oscillations due to the beating of the quantum dot and the band edge transitions.

DOI: 10.1103/PhysRevB.73.205317 PACS number(s): 73.21.La, 71.35.−y, 78.66.−w

I. INTRODUCTION

Quantum dots can be seen as the ultimate limit of quantum confinement. The translational degrees of freedom are quenched in all three directions resulting in a zero-dimensional nanostructure which can also be considered as an artificial atom. Because the coupling of the dots to the environment is relatively weak, for low excitation levels relatively long dephasing times are expected and observed by four-wave mixing (FWM),[1] particularly at low temperatures.[2] For weak excitation in the surrounding two-dimensional (2D) layer the transfer of carriers from the plasma continuum to the dot levels is at higher temperatures determined by the electron–LO-phonon interaction. Bayer and Forchel[3] measured for a single quantum dot the homogeneous linewidth for both resonant and nonresonant excitation. In the low-excitation regime they found at room temperature a dephasing time of about 220 fs. At higher excitation levels the measured relaxation time for the carrier capture process measured in terms of the rise time of the photoluminescence[4] become shorter with increasing excitation power P_{exc}, which points to Auger transitions between the 2D continuum and the dot levels. Above the threshold for the onset of Auger processes the capture time has been found to decrease as $\tau_r \propto 1/P_{exc}$ (Ref. 5) while in Ref. 6 a relaxation time has been measured which is inversely proportional to the density of the excited carriers in the quantum well. In this range the observed capture times are independent of temperature. In Ref. 7 a decrease of the Auger capture cross section with increasing quantum well carrier density has been measured and explained in terms of an increasing dot level population. Betz *et al.*[8] obtained from observations of a few quantum dots shifts of the dot ground state which depend on the delay between the pump and probe pulse. These measurements provide indirect information about the intradot relaxation process. Pulizzi *et al.*[9] studied in particular the dependence of the relaxation time on the nonresonant excitation frequency.

Bockelmann and Egeler[10] studied the carrier relaxation by Auger processes already in 1992, emphasizing that in such a treatment the continuum states and the dot states have to be orthogonalized. More detailed calculations of the relaxation and dephasing due to Auger processes have been published in Refs. 11 and 14–18. Schneider *et al.*[17] used a quantum kinetic analysis with a free-particle generalized Kadanoff-Baym ansatz, but stationary populations. All the other treatments are based on a semiclassical Markovian kinetics with an equilibrium form of the screening of the Coulomb interaction by the free carriers in the 2D layer. So far, a complete study of the time evolution of the reduced density matrix of the quantum dot after an ultrashort pulse excitation in the plasma has not been given to our knowledge.

It is known[19] that the semiclassical kinetics has to be replaced by a non-Markovian quantum kinetics if the relevant time interval, i.e., the pulse width, is comparable to or shorter than the period of a plasma or phonon oscillation. In specific cases such as the exactly solvable model with only one representative phonon mode the coherent quantum kinetic regime can extend even to time intervals considerably longer than the phonon period.[12] Thus for femtosecond excitations with intensive pulses a quantum kinetic treatment of the relaxation and dephasing is needed. On these short time scales the screened Coulomb potential cannot be taken in its equilibrium form, but has to be calculated self-consistently as a function of two times from its Dyson equation.[20] The polarization bubble will be determined in a time-dependent self-consistent random phase approximation (RPA). Because the RPA is not a conserving approximation one is faced in

the general two-time formulation with a long-wavelength divergence.[21] This problem can be avoided by using the weak-coupling generalized Kadanoff-Baym approximation[19,22] which expresses the two-time propagator $G^<(t,t')$ by a product of the retarded Green's function and the reduced density matrix,

$$G^<(t,t') = \begin{cases} -G^r(t,t')\rho(t') & \text{for } t > t', \\ \rho(t)G^a(t,t') & \text{for } t < t', \end{cases} \quad (1)$$

where G^r and G^a are the retarded and advanced Green's functions, respectively, and ρ is the density matrix. Using this approximation the two diverging contributions cancel[21] so that a well-behaved interband polarization is obtained. Dealing with the kinetics of Auger trapping processes—in which two electrons of the 2D continuum scatter one into a dot level and one up in the continuum—the trapping of an electron and a hole occur successively. Thus charged states of the quantum dot occur at least as intermediate states, although the probability, say, for a hole trapping is certainly increased if an electron is already trapped on the dot previously. The charged dots will induce surface charges and polarize the surrounding plasma. In order to describe this situation one has to deal with a spatially inhomogeneous plasma. Both the charged dot states with their Coulomb Hartree terms and the spatially inhomogeneous plasma would complicate a quantum kinetic description considerably. We will therefore disregard the effects of charged states on the quantum kinetics, which is valid—at least in a mean-field description—only for symmetric conduction and valence bands with equal electron and hole masses. Naturally for GaAs quantum dot systems the effective electron mass is about an order of magnitude smaller than the hole mass. In such an asymmetric system the electron and hole capture rates are different, resulting in charged dot states. However, electrodynamic forces will compensate these localized charges by polarizing the 2D plasma of excited carriers around the quantum dot, so that at the end more or less correlated capture processes will take place even in an asymmetric situation. In this sense it is hoped that our simplified—but consistent—model will provide results that are qualitatively similar to those for more complex realistic models.

It should be noted too that the spin degrees of freedom are not included in the present treatment. Again the electron and hole spin may have interesting influence as is known from the observed Kondo resonances in transport[23] or the observations of quantum dot trions with an electron spin singlet or triplet structure.[24]

In the following the quantum kinetic equations for the dot and the surrounding 2D plasma will be treated considering Coulomb and LO-phonon interactions in the symmetric band model. We will solve these equations for an excitation with one and two femtosecond pulses, respectively. For the two-pulse excitation we calculate the absorption spectrum of a delayed weak probe pulse for various pump pulse intensities, which yields information about the relaxation kinetics. Furthermore, we calculate the time-integrated four-wave-mixing signal and study the dephasing due to the Coulomb and LO-phonon scattering. The obtained dephasing times decrease with increasing 2D plasma densities. For short pulses a beating between plasma edge and quantum dot transitions is obtained.

II. QUANTUM KINETIC EQUATIONS FOR A DOT IN A 2D WETTING LAYER

A. The Coulomb Hamiltonian

The Hamiltonian of the considered quantum dot (D) in a quantum well or wetting layer (W) with Coulomb interaction between the carriers and the interaction with a coherent light field is

$$H = H_0 + H^{e\text{-}e} + H^{ex},$$

with the free-particle Hamiltonian (with free-particle energies ε_ν)

$$H_0 = \sum_\nu \varepsilon_\nu a_\nu^\dagger a_\nu,$$

the dipole interaction Hamiltonian with the dipole matrix element $d_{\nu\mu}$ and the amplitude $E_0(t)$ and frequency ω of the laser field,

$$H^{ex} = -\frac{1}{2}E_0(t)\sum_{\nu_1\nu_2}(d_{\nu_1\nu_2}a_{c,\nu_1}^\dagger a_{v,\nu_2}e^{-i\omega t} + \text{H.c.}),$$

and the Hamiltonian for the Coulomb interaction,

$$H^{e\text{-}e} = \frac{1}{2}\sum_{\nu_1\nu_2\nu_3\nu_4} V_{\nu_1\nu_2\nu_3\nu_4}a_{\nu_1}^\dagger a_{\nu_4}^\dagger a_{\nu_3}a_{\nu_2}.$$

The quantum numbers ν_i describe all D and W states. The Coulomb matrix elements are given by

$$\begin{aligned} V_{\nu_1\nu_2\nu_3\nu_4} &= \int d^3r_1 d^3r_2 \Phi_{\nu_1}^*(r_1)\Phi_{\nu_4}^*(r_2)V(r_1-r_2)\Phi_{\nu_3}(r_1)\Phi_{\nu_2}(r_2) \\ &= \sum_q V_{n_1n_2n_3n_4}^{b_1b_2}(q)\delta_{b_1b_3}\delta_{b_2b_4}\int d^2\rho_1 \phi_{l_1}^{b_1}(\rho_1)^* e^{-iq\rho_1}\phi_{l_3}^{b_3} \\ &\quad \times(\rho_1)\int d^2\rho_2 \phi_{l_4}^{b_4}(\rho_2)^* e^{iq\rho_2}\phi_{l_2}^{b_2}(\rho_2). \end{aligned} \quad (2)$$

Here n_i and l_i are the quantum numbers for the z-dependent part and the in-plane components of the wave functions, and b_i is the band index. The in-plane Coulomb matrix elements are[28]

$$\begin{aligned} V_{n_1n_2n_3n_4}^{b_1b_2}(q) &= V_{2D}(q)\int dz_1 dz_2 \xi_{n1}^{b_1}(z_1)^*\xi_{n4}^{b_2}(z_2)^* \\ &\quad \times e^{-q|z_1-z_2|}\xi_{n3}^{b_1}(z_1)\xi_{n2}^{b_2}(z_2), \end{aligned} \quad (3)$$

where V_{2D} is the 2D Fourier transformation of the Coulomb potential.

Considering this Hamiltonian, we assume only one state per dot for the electron and hole, respectively. This assumption is certainly a strong idealization, but small quantum dots with a relatively weak confinement potential have only very

few levels. In particular natural quantum dots[25] that occur at interface fluctuations of narrow quantum wells are dots in which a single exciton transition is well resolved.[26] Other few-level dot systems occur in self-assembled InGaAs quantum dots.[27]

As discussed above, a completely symmetric model will be treated for electrons and holes in the plasma and also in the dot in order to avoid charged states. A coupling between different dots is not taken into account.

Assuming the dots are contained in W with infinitely potential barriers, the in-plane Coulomb matrix elements are identical and can be computed analytically:

$$V(q) = \frac{8\pi e^2}{\epsilon_0 A q}\left(\frac{8\pi^4(e^{-L_z q}+L_z q-1)+5\pi^2 L_z^3 q^3+3L_z^5 q^5/4}{L_z^2 q^2(4\pi^2+L_z^2 q^2)^2}\right). \tag{4}$$

B. Orthogonalization of the wave functions

Before we can continue with the derivation of the quantum kinetic equations we have to orthogonalize the quantum dot and quantum well wave functions.[10,11,14] The 2D plane wave $\phi_k(\rho)$ is orthogonalized to the quantum dot state ϕ_d with

$$|\phi_k\rangle = \frac{1}{N_k}(|\phi_k^0\rangle - \langle\phi_d|\phi_k^0\rangle|\phi_d\rangle). \tag{5}$$

N_k is a normalization factor, and $\phi_k^0 = e^{ik\rho}/\sqrt{A}$ is the 2D plane wave state in the absence of the QD, where A is the normalization area of the quantum well. If an ensemble average over random dot positions is taken, the renormalized[14] 2D states remain orthogonal to each other.

C. Derivation of the quantum kinetics

We will derive the quantum kinetic equations for the reduced density matrix from the Dyson equation of the electron propagator $G^<(t,t')$ following the procedure described in Ref. 19. These propagators which describe the kinetics are defined as

$$G^<_{\nu_1\nu_2}(t_1,t_2) = \frac{i}{\hbar}\langle a^\dagger_{\nu_2}(t_2)a_{\nu_1}(t_1)\rangle,$$

$$G^>_{\nu_1\nu_2}(t_1,t_2) = -\frac{i}{\hbar}\langle a_{\nu_1}(t_1)a^\dagger_{\nu_2}(t_2)\rangle. \tag{6}$$

The band off-diagonal elements of $G^{b_1 b_2}_{DW}$ will be neglected. Spatial homogeneity has been assumed so that $G_{k_1k_2} = \delta_{k1,k2}G_{k_1}$.

The equation of motion for the propagators in the equal-time limit can be written as

$$\frac{\partial}{\partial t}G^<_{\nu_1\nu_2}(t,t) = \left.\frac{\partial}{\partial t}G^<_{\nu_1\nu_2}(t,t)\right|_{coh} + \left.\frac{\partial}{\partial t}G^<_{\nu_1\nu_2}(t,t)\right|_{scatt}, \tag{7}$$

where the coherent part is given by the free evolution and a mean-field contribution due to the Coulomb exchange interaction and the interaction with the coherent light field:

$$\left.\frac{\partial}{\partial t}G^<_{\nu_1\nu_2}(t,t)\right|_{coh} = -\frac{i}{\hbar}(\varepsilon_{\nu_1}-\varepsilon_{\nu_2})G^<_{\nu_1\nu_2}(t,t) - \frac{i}{\hbar}\sum_{\nu_3}[\Sigma^\delta_{\nu_1\nu_3}(t)G^<_{\nu_3\nu_2}(t,t) - G^<_{\nu_1\nu_3}(t,t)\Sigma^\delta_{\nu_3\nu_2}(t)], \tag{8}$$

with the instantaneous mean-field self-energy

$$\Sigma^\delta_{\nu_1\nu_3}(t) = \Sigma_{ex}+\Sigma^{HF} = -dE(t)(1-\delta_{\nu_1\nu_2}) + i\hbar V_{\nu_1\nu_2\nu_3\nu_4}G^<_{\nu_3\nu_4}(t,t). \tag{9}$$

The scattering part can be expressed in terms of the scattering self-energies $\sigma^<$ and $\sigma^>$,

$$\left.\frac{\partial}{\partial t}G^<_{\nu_1\nu_2}(t,t)\right|_{scatt} = -\frac{i}{\hbar}\sum_{\nu_3}\int_{-\infty}^{t}dt'[\sigma^>_{\nu_1\nu_3}(t,t')G^<_{\nu_3\nu_2}(t',t) - \sigma^<_{\nu_1\nu_3}(t,t')G^>_{\nu_3\nu_2}(t',t) - G^>_{\nu_1\nu_3}(t,t')\sigma^<_{\nu_3\nu_2}(t',t) + G^<_{\nu_1\nu_3}(t,t')\sigma^>_{\nu_3\nu_2}(t',t)], \tag{10}$$

where the scattering self-energy will be taken in the self-consistent GW approximation with a two-time-dependent screened Coulomb scattering potential $v^<$ and $v^>$ and with a phonon propagator $D^<$ and $D^>$:

$$\sigma^{(>)}_{\nu_1\nu_2}(t,t') = i\hbar\sum_{\nu_3\nu_4}[v^{(<)}_{\nu_1\nu_2\nu_3\nu_4}(t',t) + g_{\nu_1,\nu_3}D^{(<)}_{\nu_1\nu_2\nu_3\nu_4} \times(t',t)g_{\nu_4,\nu_2}]G^{(>)}_{\nu_3\nu_4}(t,t'). \tag{11}$$

The matrix elements for the interaction of electrons and LO phonons are denoted as g_{ν_1,ν_2}. Note that for simplicity we have neglected the screening for the electron-phonon self-energy.

D. Screened coulomb potential

The screened Coulomb potential has to be calculated from its Dyson equation:

$$w_{\nu_1\nu_2\nu_3\nu_4}(t,t') = V_{\nu_1\nu_2\nu_3\nu_4}(t-t') + \sum_{\nu_i}\int dt_1 dt_2 V_{\nu_8\nu_2\nu_5\nu_4} \times(t-t_1)L_{\nu_5\nu_6\nu_7\nu_8}(t_1,t_2)w_{\nu_1\nu_7\nu_3\nu_6}(t_2,t'), \tag{12}$$

where L is the polarization function, which in the time-dependent RPA is given by

$$L_{\nu_1\nu_2\nu_3\nu_4}(t,t') = -i\hbar c_1 G_{\nu_1\nu_2}(t,t')G_{\nu_3\nu_4}(t',t) \tag{13}$$

and the Coulomb matrix elements for the screened interaction

$$w_{\nu_1\nu_2\nu_3\nu_4} = \int d^3r_1 d^3r_2 \Phi^*_{\nu_1}(r_1)\Phi^*_{\nu_4}(r_2) w(r_1,r_2)\Phi_{\nu_3}(r_1)\Phi_{\nu_2}(r_2)$$
$$= \sum_q w^{b_1b_2}_{n_1n_2n_3n_4}(q)\,\delta_{b_1b_3}\delta_{b_2b_4}\langle\phi^{b_1}_{l_1}|e^{-iq\cdot\rho_1}|\phi^{b_3}_{l_3}\rangle \times\langle\phi^{b_4}_{l_4}|e^{iq\cdot\rho_1}|\phi^{b_2}_{l_2}\rangle \quad (14)$$

with the in-plane matrix elements

$$w^{b_1b_2}_{n_1n_2n_3n_4}(q) = \int dz_1 dz_2 \xi^{b_1}_{n_1}(z_1)^*\xi^{b_2}_{n_4}(z_2)^* w(q,z_1,z_2) \times\xi^{b_1}_{n_3}(z_1)\xi^{b_2}_{n_2}(z_2). \quad (15)$$

We assume in the following that the screening is solely due to the 2D carriers. We then obtain the Dyson equation for the in-plane matrix elements:

$$w(q,t,t') = V(q,t-t') + \int dt_1 dt_2 V \times(q,t-t_1)L(q,t_1,t_2)w(q,t_2,t'),$$

where $L(q,t_1,t_2)$ is given by

$$L(q,t_1,t_2) = -i\hbar c_1 \sum_{k,b_1b_2} G^{b_1b_2}_k(t_1t_2)G^{b_2b_1}_{k-q}(t_2t_1)|F_{\vec{k},\vec{k}-\vec{q}}|^2. \quad (16)$$

Here F is defined by

$$\langle\phi_k|e^{iq\cdot\rho}|\phi_{k'}\rangle = \int d^2\rho\ \phi_{\vec{k}}(\rho)^* e^{iq\rho}\phi_{\vec{k}'}(\rho) = \delta_{\vec{k}-\vec{q}-\vec{k}'}F_{\vec{k},\vec{k}'}. \quad (17)$$

The Coulomb matrix elements are calculated through

$$w_{\nu_1\nu_2\nu_3\nu_4}(t,t') = \sum_q w(q,t,t')\langle\phi_{l_1}|e^{-iq\cdot\rho}|\phi_{l_3}\rangle\langle\phi_{l_4}|e^{iq\cdot\rho}|\phi_{l_2}\rangle. \quad (18)$$

E. Phonon propagators

We will assume that the optical phonons are those of the bulk GaAs medium. With this approximation we disregard localized phonon modes around the quantum well layer and in particular around the quantum dot. It is known that these evanescent modes reduce the number of freely traveling modes and that the remaining plane wave modes together with the evanescent modes have in total a comparable effect on the electrons as the unperturbed bulk modes. It is further assumed that the LO phonons form a thermal heat bath. With this approximation we neglect the effects of coherent phonon modes and polaron effects. This assumption seems justified if the areal dot density is low and if the polaron coupling is weak as is the case for GaAs-type materials. However, an exactly solvable model in which the phonons are represented as a single Einstein oscillator[12] has shown that nonthermal phonons play an important role if the pulse width is of the same order as the phonon period. Magneto-optical studies of Hameu *et al.*[13] suggest that in quantum dot systems strong-coupling polaron effects may be present even for weak Fröhlich coupling constants. In II-VI compound quantum dot systems the polaron effects are stronger and require one to treat also the quantum kinetic equations for the LO phonons (see, e.g., Refs. 14 and 16). We are not addressing the effects of nonthermal phonons because in our studies the pulse width is much shorter than the phonon period. Polaron effects are also omitted because in our treatment we consider weak-coupling materials and because the phonon scattering kinetics is only used to supplement the dominating Coulomb kinetics, e.g., by providing a cooling mechanism which carrier-carrier scattering alone cannot provide.

In analogy with the Coulomb potential discussed above, the phonon propagators of (11) and the interaction matrix elements are

$$g_{\nu_1,\nu_3}D^{(<,>)}_{\nu_1\nu_2\nu_3\nu_4}(t',t)g_{\nu_4,\nu_2} = \sum_q g_q^2 D^{(<,>)}(q,t,t')\langle\phi_{l_1}|e^{-iq\cdot\rho}|\phi_{l_3}\rangle \times\langle\phi_{l_4}|e^{iq\cdot\rho}|\phi_{l_2}\rangle, \quad (19)$$

with the free-phonon propagators[19]

$$D^<(q,t,t') = -i\sum_{\pm} N_q^{\pm}e^{\pm i\omega_0(t-t')} \quad \text{and}$$

$$D^>(q,t,t') = -D^<(q,t,t')^*, \quad (20)$$

where $N_q^{\pm}=N+\frac{1}{2}\pm\frac{1}{2}$ with the Bose phonon distribution $N=1/(e^{\omega_0/k_BT}-1)$. The Fröhlich interaction matrix element is given by

$$g_q^2 = \frac{\hbar\omega_0}{2}\left(\frac{\epsilon_0}{\epsilon_\infty}-1\right)V_q, \quad (21)$$

where V_q is given in (4). For GaAs this polar coupling is rather weak, corresponding to a dimensionless polaron coupling constant of $\alpha=0.06$. Note that we now use the screening constant ϵ_∞ in the Coulomb potential because the LO phonons are treated explicitly.[28]

F. Final quantum kinetic equations

The resulting quantum kinetic equations take the following forms.

Coherent part.

$$\left.\frac{\partial}{\partial t}G^<_{m,cv}(t,t)\right|_{coh} = -\frac{i}{\hbar}[e_{m,c}(t)-e_{m,v}(t)]G^<_{m,cv}(t,t) + i\Omega_m(t) \times[G^<_{m,vv}(t,t)-G^<_{m,cc}(t,t)],$$

$$\left.\frac{\partial}{\partial t}G^<_{m,cc}(t,t)\right|_{coh} = -\mathrm{Im}[i\Omega_m(t)G^<_{m,cv}(t,t)^*], \quad (22)$$

where the subscript m refers to either quantum well (labeled by vector k) or quantum dot (denoted by 0) states, and the renormalized energies

$$e_{0,b}(t) = \epsilon_{0,b} + i\hbar V_{00kk}\left(\frac{\delta_{bv}}{i\hbar} + G^{<}_{k,bb}(t,t)\right) \quad (b = c,v),$$

$$e_{kb}(t) = \epsilon_{\vec{k}b} + i\hbar\sum_{k'} V_{kkk'k'}\left(\frac{\delta_{bv}}{i\hbar} + G^{<}_{k',bb}(t,t)\right) + i\hbar V_{kk,00}\left(\frac{\delta_{bv}}{i\hbar} + G^{<}_{0,bb}(t,t)\right)$$

and the renormalized Rabi frequencies

$$\hbar\Omega_0(t) = dE(t) - i\hbar V_{00,kk}G^{<}_{k,cv}(t,t),$$

$$\hbar\Omega_k(t) = dE(t) - i\hbar\sum_{k'} V_{kkk'k'}G^{<}_{k',cv}(t,t) - i\hbar V_{kk00}G^{<}_{0,cv}(t,t)$$

are introduced.

Scattering part. Note that the scattering part contains two-time-dependent propagators and self-energies. Thus the kinetic equation is not closed as it should be:

$$\begin{aligned}\frac{\partial}{\partial t}G^{<}_{0,b_1b_2}(t,t)\bigg|_{scatt} &= -\frac{i}{\hbar}\sum_{b_3}\int_{-\infty}^{t} dt'[\sigma^{>}_{0,b_1b_3}(t,t')G^{<}_{0,b_3b_2}(t',t) \\ &- \sigma^{<}_{0,b_1b_3}(t,t')G^{>}_{0,b_3b_2}(t',t) - G^{>}_{0,b_1b_3}(t,t')\sigma^{<}_{0,b_3b_2}(t',t) \\ &+ G^{<}_{0,b_1b_3}(t,t')\sigma^{>}_{0,b_3b_2}(t',t)], \end{aligned} \tag{23}$$

$$\begin{aligned}\frac{\partial}{\partial t}G^{<}_{\vec{k},b_1b_2}(t,t)\bigg|_{scatt} &= -\frac{i}{\hbar}\sum_{b_3}\int_{-\infty}^{t} dt'[\sigma^{>}_{\vec{k},b_1b_3}(t,t')G^{<}_{\vec{k},b_3b_2}(t',t) \\ &- \sigma^{<}_{\vec{k},b_1b_3}(t,t')G^{>}_{\vec{k},b_3b_2}(t',t) - G^{>}_{\vec{k},b_1b_3}(t,t')\sigma^{<}_{\vec{k},b_3b_2}(t',t) \\ &+ G^{<}_{\vec{k},b_1b_3}(t,t')\sigma^{>}_{\vec{k},b_3b_2}(t',t)]. \end{aligned} \tag{24}$$

The scattering self-energies σ are given by

$$\sigma^{(\substack{>\\<})}_{0,b_1b_3}(t,t') = i\hbar\sum_{k_1} w^{(\substack{>\\<})}_{00k_1k_1}(t,t')G^{(\substack{<\\>})}_{k_1,b_1b_2}(t,t')$$

and

$$\sigma^{(\substack{>\\<})}_{k,b_1b_3}(t,t') = i\hbar\sum_{k_1} w^{(\substack{>\\<})}_{kkk_1k_1}(t,t')G^{(\substack{<\\>})}_{k_1,b_1b_2}(t,t') + w^{(\substack{>\\<})}_{kk00}(t,t')G^{(\substack{<\\>})}_{0,b_1b_2}(t,t').$$

As mentioned above we will use the generalized Kadanoff-Baym approximation in order to express the two-time propagators in terms of spectral Green's functions and the reduced density matrix:

$$G^{<}_{k,0}(t,t') \simeq -G^{r}_{k,0}(t,t')\rho_{k,0}(t') \quad \text{for} \quad t \geqslant t', \tag{25}$$

with

$$G^{r}_{k,0}(t,t') \simeq -\frac{i}{\hbar}\Theta(t-t')e^{-(i/\hbar)\epsilon_{k,0}(t-t')}.$$

In the following the ground-state wave function of the dot $\phi_0(\rho) = \beta/\sqrt{\pi}e^{-(1/2)\beta^2\rho^2}$ are used in the orthogonalization of the wave functions and in the calculation of the Coulomb matrix elements. Here β is given by $\beta_{e,h} = \sqrt{m_{e,h}E^{e,h}_{HO}/\hbar^2}$ (Ref. 11), where $E^{e,h}_{HO}$ is the energy difference between the localized electron (hole) and the continuum. The orthogonalized wave function takes the form $\phi_k(\rho) = 1/N_k[e^{i\vec{k}\cdot\vec{\rho}} - 2\alpha(k)e^{-(1/2)\beta^2\rho^2}]$ with $\alpha(k) = e^{-k^2/(2\beta^2)}$ and $N_k = \sqrt{1 - N|\langle\phi^0_k|\phi_0\rangle|^2}$ with the number of quantum dots N. We get then the Coulomb matrix elements

$$\begin{aligned} w_{00kk}(t,t') = \frac{4\pi N}{\beta^2 N_k^2 A}\sum_q w(q,t,t')[&\alpha(\vec{k}-\vec{q})^2 \\ &+ \alpha(k)^2 e^{-q^2/(2\beta^2)} - 2\alpha(k)\alpha(\vec{k}-\vec{q})e^{-q^2/(4\beta^2)}] \end{aligned} \tag{26}$$

and

$$\begin{aligned} w_{k_1k_1k_3k_3}(t,t') &= w(k_3-k_1,t,t')|F_{k_1,k_3}|^2 \\ &= \frac{1}{N_{k_1}N_{k_3}}w(k_3-k_1,t,t') \\ &\times\left(1 - \frac{2\pi N}{\beta^2 A}\alpha(k_1)^2 - \frac{2\pi N}{\beta^2 A}\alpha(k_3)^2 + \frac{2\pi N}{\beta^2 A}\alpha(k_1)\alpha(k_3)e^{-(k_3-k_1)^2/4\beta^2}\right)^2. \end{aligned} \tag{27}$$

Note that in the large limit N/A remains constant and will be replaced by the quantum dot density n_D. With these formulas the kinetic equations are closed provided the spectral Green's functions $G^r(t,t')$ and $G^a(t,t')$ can be taken in the simple free-particle approximation (26).

III. NUMERICAL RESULTS

In the following we will use first a single femtosecond laser pulse in order to study the general features of the calculated density matrix of the dot. In order to make predictions for two-pulse experiments, we will consider both differential transmission spectroscopy and four-wave-mixing type setups.

A. Excitation with a single femtosecond pulse

We assume a 20 fs Gauss pulse tuned to the band edge of the 2D continuum. The dot obtains the electron and hole via Coulomb Auger processes and scattering processes with phonon emission. The lattice temperature is assumed to be $T = 300$ K. All material parameters are taken for GaAs except that we treat equal band masses $m_h = m_e = 0.098m_0$. With these equal masses the exciton Bohr radius is that of GaAs. The dot levels are assumed to be $E_{HO} = 27.5$ meV below the conduction and above the valence band edge, respectively.

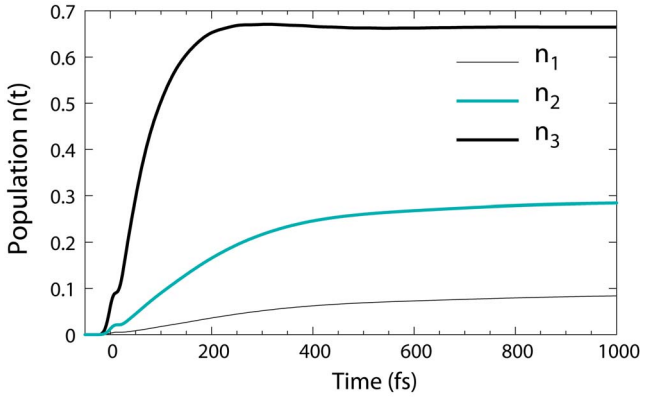

FIG. 1. (Color online) Computed distribution function for a quantum dot. $n_1=0.45\times10^{11}$ cm^{-2}, $n_2=2.0\times10^{11}$ cm^{-2}, and $n_3=8.5\times10^{11}$ cm^{-2}.

The 2D density of quantum dots in the well is $n_D=0.5\times10^{11}$ cm^{-2}.

In Fig. 1 we see the evolution of the dot populations $n_e=n_h=n$ for three excitation intensities. The steady state of the dot population is reached faster at higher plasma densities as one would have assumed. At the lowest density n_1 it takes about 800 fs to reach steady state, while at the highest density n_3 it takes only about 200 fs.

The off-diagonal matrix elements of the density matrix, which yield the optically induced polarization of the dot, are shown in Fig. 2 for four excitation intensities. The dot polarization follows closely the pump pulse. After about 50 fs the decay of the remaining polarization is superimposed by beating oscillations whose period is given by the energetic difference between the band gap and the energy difference between the two dot levels. At the highest excitation intensity these beats are lost; instead a sharp minimum occurs indicating a nearly complete Rabi flop. The beating oscillations disappear for laser pulses with duration larger than 60 fs.

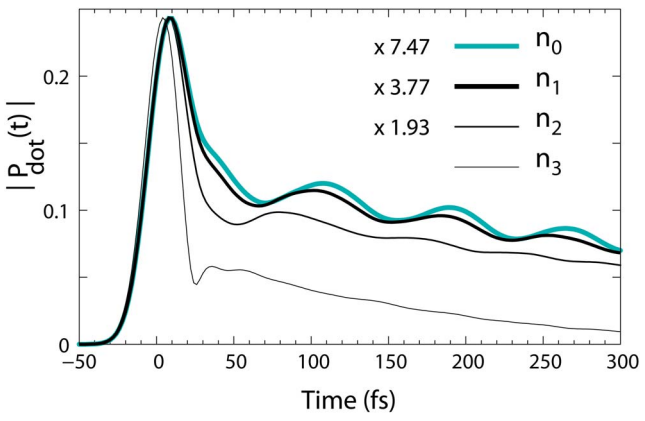

FIG. 2. (Color online) Polarization function for a quantum dot. The numbers show by what factor the corresponding polarization curve has been multiplied. The steady-state plasma densities after the pump pulse are $n_0=0.45\times10^{10}$ cm^{-2}, $n_1=0.45\times10^{11}$ cm^{-2}, $n_2=2.0\times10^{11}$ cm^{-2}, and $n_3=8.5\times10^{11}$ cm^{-2}.

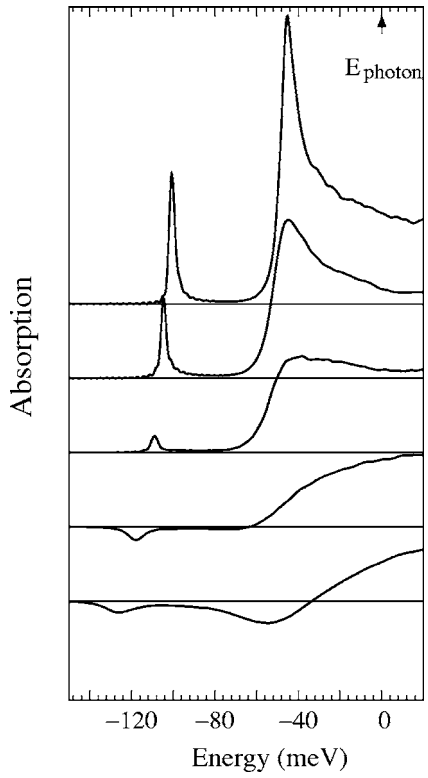

FIG. 3. Absorption spectrum for densities $n=0.45\times10^{11}$ cm^{-2}, $n=2.0\times10^{11}$ cm^{-2}, $n=4.0\times10^{11}$ cm^{-2}, $n=8.5\times10^{11}$ cm^{-2}, and $n=1.1\times10^{12}$ cm^{-2}.

B. Simulations for excitations with two femtosecond pulses

While the response to one pulse only yields a first qualitative insight, one can get much closer to actual experiments by considering a pump pulse followed by a delayed probe pulse. We will first calculate the absorption spectrum of a weak test pulse delayed by 200 fs with respect to the strong pump pulse. The width of the pump pulse was again 20 fs, while the test pulse has been assumed to be 10 fs to get sufficient spectral width. Figure 3 shows the absorption spectra for various stationary plasma densities of the dot and the higher-lying 2D continuum again for the symmetric band model. At the two lowest densities one sees the considerable excitonic enhancement of the band edge and the redshifting absorption line of the dot. Such redshifts with increasing pump intensity have been observed in luminescence.[29] A corresponding redshift of the dot absorption line has been calculated before by Schneider *et al.*[17] in a time- and frequency-dependent formulation of quantum kinetics. At the highest densities gain develops both below the dot line and below the band edge of the continuum.

The delay time dependence of the absorption spectra is shown in Fig. 4 at a steady-state plasma density of $n=8.5\times10^{11}$ cm^{-2}. One sees that the original dot absorption changes after slightly more than 100 fs into gain, while at that time the gain of the continuum is not yet developed.

Finally we calculate for two equally strong pulses traveling in the directions $\vec{k}_1$ and $\vec{k}_2$ the FWM signal by projecting out the polarization in the direction $2\vec{k}_2-\vec{k}_1$ with the technique described, e.g., in Ref. 19. The calculated time-

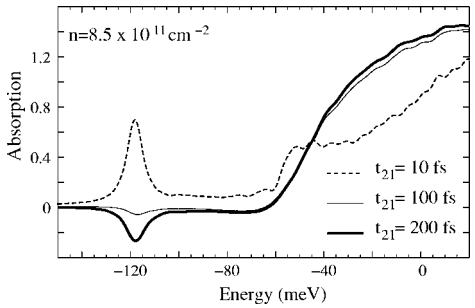

FIG. 4. Absorption spectrum for the density $n=8.5\times10^{11}$ cm^{-2} for three delay times $t_{21}=10$ fs, $t_{21}=100$ fs, and $t_{21}=200$ fs.

integrated FWM signal is shown for four steady-state plasma densities in Fig. 5. After a steep decay one sees an approximately exponential decay with the dephasing times of 170, 135, 74, and 35 fs for the increasing excited densities n_0, n_1, n_2, and n_3. The dephasing time of 170 fs at the lowest considered density is mainly determined by LO-phonon scattering and may approach about 200 fs in the limit of very low intensities. A phonon dephasing time of about 250 fs has been measured by Borri *et al.*[1] for resonant excitation, where the role of the wetting layer is of minor influence. One has to

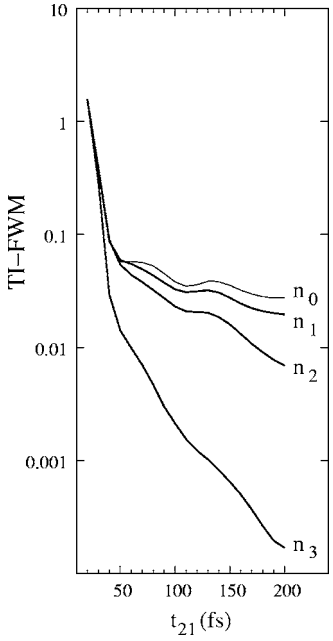

FIG. 5. Time-integrated four-wave-mixing signals for densities $n_0=0.10\times10^{11}$ cm^{-2}, $n_1=0.45\times10^{11}$ cm^{-2}, $n_2=2.00\times10^{11}$ cm^{-2}, and $n_3=8.50\times10^{11}$ cm^{-2}.

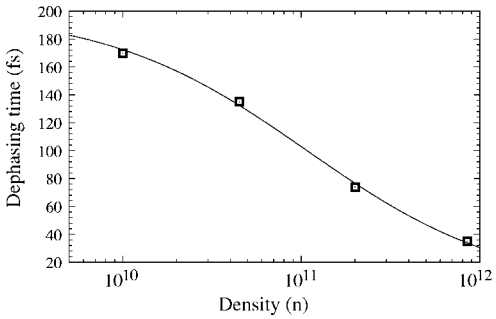

FIG. 6. Dephasing time τ versus density n.

consider that the dephasing time decreases with increasing detuning frequency for nonresonant excitation as shown by Bayer and Forchel.[3] For high temperatures they obtained for resonant excitation again a dephasing time of the order of 200 fs. Dephasing times similar to the measured ones have been calculated by Uskov *et al.*[30] also for resonant excitation.

The inverse density-dependent dephasing time can be written as a power law $1/\tau=1/\tau_0+cn^x$ as seen from Fig. 6. The constants of the best fit are $\tau_0\simeq200$ fs, $c=3.2\times10^{-9}$, and an exponent $x=0.77$. The result resembles the density-dependent relaxation time (not dephasing time) measured by Morris *et al.*[6] in the form $1/\tau_r\propto n$. Superimposed on the FWM signal of Fig. 5 are the beating oscillations of the band edge and dot transitions. At the highest density the beating oscillations are nearly lost.

In conclusion, we have investigated the quantum kinetics of a dot embedded in a 2D continuum with time-dependent screened Coulomb interaction and phonon scattering. We have calculated the resulting density matrix after a 20 fs pulse excitation and studied the femtosecond dynamics of the dot polarization dephasing and the buildup of the dot population for Auger and phonon processes coupling the continuum and the dot. For two-pulse excitation configurations, we have calculated the absorption spectra of the delayed weak test pulse and shown how the original absorption spectra of the dot and the continuum change into gain spectra at high excitation levels. Finally the FWM signal has been calculated yielding dephasing times which decrease increasing excitation intensity in the range from 170 to 35 fs at the highest intensities. Superimposed on the decaying FWM signal oscillations have been obtained due to the beating of band edge and dot transitions.

ACKNOWLEDGMENTS

The work has been supported by the DFG and BMBF. The calculations have been performed at the Frankfurt Center of Scientific Computing.

[1] P. Borri, W. Langbein, J. Mork, J. M. Hvam, F. Heinrichsdorff, M. H. Mao, and D. Bimberg, Phys. Rev. B **60**, 7784 (1999).

[2] P. Borri, W. Langbein, S. Schneider, U. Woggon, R. L. Sellin, D. Ouyang, and D. Bimberg, Phys. Rev. Lett. **87**, 157401 (2001).

[3] M. Bayer and A. Forchel, Phys. Rev. B **65**, 041308(R) (2002).

[4] B. Ohnesorge, M. Albrecht, J. Oshinowo, A. Forchel, and Y. Arakawa, Phys. Rev. B **54**, 11532 (1996).

[5] S. Sanguinetti, K. Watanabe, T. Taneno, M. Wakaki, N. Koguchi,

T. Kuroda, F. Minami, and M. Gurioli, Appl. Phys. Lett. **81**, 613 (2002).
[6] D. Morris, N. Perret, and S. Fafard, Appl. Phys. Lett. **75**, 3593 (1999).
[7] S. Raymond, K. Hinzer, S. Fafard, and J. L. Merz, Phys. Rev. B **61**, R16331 (2000).
[8] M. Betz, S. Trumm, A. Leitenstorfer, E. Beham, H. Kenner, M. Bichler, A. Zrenner, and G. Abstreiter, Phys. Status Solidi B **233**, 401 (2002).
[9] F. Pulizzi, A. J. Kent, A. Pantane, L. Eaves, and M. Henini, Appl. Phys. Lett. **84**, 3046 (2004).
[10] U. Bockelmann and T. Egeler, Phys. Rev. B **46**, 15574 (1992).
[11] H. C. Schneider, W. W. Chow, and S. W. Koch, Phys. Rev. B **64**, 115315 (2001).
[12] V. M. Axt, M. Herbst, and T. Kuhn, Superlattices Microstruct. **26**, 117 (1999).
[13] S. Hameau, Y. Guldner, O. Verzelen, R. Ferreira, G. Bastard, J. Zeman, A. Lemaitre, and J. M. Gerard, Phys. Rev. Lett. **83**, 4152 (1999).
[14] T. R. Nielsen, P. Gartner, and F. Jahnke, Phys. Rev. B **69**, 235314 (2004).
[15] W. W. Chow, H. C. Schneider, and M. C. Phillips, Phys. Rev. A **68**, 053802 (2003).
[16] J. Seebeck, T. R. Nielsen, P. Gartner, and F. Jahnke, Phys. Rev. B **71**, 125327 (2005).
[17] H. C. Schneider, W. W. Chow, and S. W. Koch, Phys. Rev. B **70**, 235308 (2004).
[18] R. Wetzler, A. Wacker, and E. Scholl, J. Appl. Phys. **95**, 7966 (2004).
[19] H. Haug and A. P. Jauho, *Quantum Kinetics for Transport and Optics in Semiconductors* (Springer, Berlin, 1996).
[20] L. Banyai, Q. T. Vu, B. Mieck, and H. Haug, Phys. Rev. Lett. **81**, 882 (1998).
[21] P. Gartner, L. Banyai, and H. Haug, Phys. Rev. B **62**, 7116 (2000).
[22] P. Lipavsky, V. Spicka, and B. Velicky, Phys. Rev. B **34**, 6933 (1986).
[23] S. M. Cronenwett, T. H. Oosterkamp, and L. P. Kouwenhoven, Science **281**, 540 (1998).
[24] M. Bayer *et al.*, Phys. Rev. B **65**, 195315 (2002).
[25] A. Zrenner, L. V. Butov, M. Hagn, G. Abstreiter, G. Bohm, and G. Weimann, Phys. Rev. Lett. **72**, 3382 (1994).
[26] T. Unold, K. Mueller, C. Lienau, T. Elsaesser, and A. D. Wieck, Phys. Rev. Lett. **92**, 157401 (2004).
[27] P. Hawrylak, G. A. Narvaez, M. Bayer, and A. Forchel, Phys. Rev. Lett. **85**, 389 (2000).
[28] H. Haug and S. W. Koch, *Quantum Theory of the Optical and Electronic Properties of Semiconductors*, 4th ed. (World Scientific, Singapore, 2004).
[29] K. Matsuda, K. Ikeda, T. Saiki, H. Saito, and K. Nishi, Appl. Phys. Lett. **83**, 2250 (2003).
[30] A. V. Uskov, A. P. Jauho, B. Tromborg, J. Mork, and R. Lang, Phys. Rev. Lett. **85**, 1516 (2000).